Manuscript title

Lysyl oxidase regulates epithelial differentiation and barrier integrity in eosinophilic esophagitis

Short Title

LOX restores epithelial homeostasis in EoE

Authors

Masaru Sasaki[1], Takeo Hara[1], Joshua X. Wang[1], Yusen Zhou[2], Kanak V. Kennedy[1], Nicole N. Umeweni[1], Maiya A. Alston[1], Zachary C. Spergel[1], Ritsu Nakagawa[1], Emily A. Mcmillan[1], Kelly A. Whelan[3,4], Tatiana A. Karakasheva[1], Kathryn E. Hamilton[1,5], Melanie A. Ruffner[5,6], and Amanda B. Muir[1,5]

Authors' affiliations

1 Division of Gastroenterology, Hepatology, and Nutrition, The Children's Hospital of Philadelphia, Philadelphia, Pennsylvania, USA

2 Department of Biomedical and Health Informatics, The Children's Hospital of Philadelphia, Philadelphia, Pennsylvania, USA

3 Fels Cancer Institute for Personalized Medicine, Temple University Lewis Katz School of Medicine, Philadelphia, Pennsylvania, USA

4 Department of Cancer & Cellular Biology, Temple University Lewis Katz School of Medicine, Philadelphia, Pennsylvania, USA

5 Department of Pediatrics, Perelman School of Medicine, University of Pennsylvania, Philadelphia, Pennsylvania, USA

6 Division of Allergy and Immunology, The Children's Hospital of Philadelphia, Philadelphia, Pennsylvania, USA

Grant Support

This work was supported by National Institutes of Health (NIH) grants, R01DK121159 (K.A.W.), K08AI148456 (M.A.R.), R03DK118310, and R01DK124266-01 (A.B.M.); University of Pennsylvania Transdisciplinary Awards Program in Translational Medicine and Therapeutics (A.B.M.); and the Children's Hospital of Philadelphia Gastrointestinal Epithelial Modeling Program (T.A.K., and A.B.M.). This work was supported by P30DK050306: Center for Molecular Studies in Digestive and Liver Diseases.

Abbreviations

ALI, air-liquid interface; BMP, bone morphogenetic protein; DAPI, 4′,6-diamidino-2-phenylindole; DEG, differentially expressed gene; EoE, eosinophilic esophagitis; FST, follistatin; GFP, Green fluorescent protein; GSEA, Gene Set Enrichment Analysis; H&E, hematoxylin and eosin; IL, interleukin; KSFM, keratinocyte-serum free medium; LOX, lysyl oxidase; OFR, organoid formation rate; PDO, patient-derived organoid; PID, Pathway Interaction Database; p-SMAD1/5/9, phospho-SMAD1/5/9; qRT-PCR, quantitative reverse transcription-polymerase chain reaction; TEER, transepithelial electrical resistance; TGFβ, transforming growth factor-β; UMAP, uniform manifold approximation and projection; 3D, 3-dimensional

Correspondence

Amanda B. Muir, Perlman School of Medicine, University of Pennsylvania, Abramson Research Center 902E, 3615 Civic Center Boulevard, Philadelphia, PA 19104, USA. Phone: +1(215)590-3630; Fax: +1(215)590-3606; E-mail: MUIRA@chop.edu

Disclosures

Amanda B. Muir has served on the medical advisory boards for Nexstone Immunology and Bristol Meyers Squib. The rest of the authors have declared that no conflict of interest exists.

Word count

3011 words

Author Contributions

MS, TH, TAK, and ABM were responsible for the study concept and design. MS, JXW, KVK, ZCS, and RN performed the experiments. MS, TH, JXW, YZ, and KVK performed the data analyses. MS and NNU created the schematics. MAA and EAM provided reagents. MS, YZ, TAK, and ABM wrote the original draft, and MS, KAW, TAK, KEH, MAR, and ABM edited it. All authors discussed the results and reviewed the manuscript.

Data Transparency

The data and materials described in this study will be made available upon request.

Synopsis

71 Lysyl oxidase (LOX) re-established impaired epithelial homeostasis via activation of
72 BMP pathway in esophagus. The LOX/BMP axis may be a promising approach for
73 eosinophilic esophagitis.
74
75

Abstract

Background & Aims

Epithelial disruption in eosinophilic esophagitis (EoE) encompasses both impaired differentiation and diminished barrier integrity. We have shown that lysyl oxidase (LOX), a collagen cross-linking enzyme, is upregulated in the esophageal epithelium in EoE. However, the functional roles of LOX in the esophageal epithelium remains unknown.

Methods

We investigated roles for LOX in the human esophageal epithelium using 3-dimensional organoid and air-liquid interface cultures stimulated with interleukin (IL)-13 to recapitulate the EoE inflammatory milieu, followed by single-cell RNA sequencing, quantitative reverse transcription-polymerase chain reaction, western blot, histology, and functional analyses of barrier integrity.

Results

Single-cell RNA sequencing analysis on patient-derived organoids revealed that LOX was induced by IL-13 in differentiated cells. LOX-overexpressing organoids demonstrated suppressed basal and upregulated differentiation markers. Additionally, LOX overexpression enhanced junctional protein genes and transepithelial electrical resistance. LOX overexpression restored the impaired differentiation and barrier function, including in the setting of IL-13 stimulation. Transcriptome analyses on LOX-overexpressing organoids identified enriched bone morphogenetic protein (BMP) signaling pathway compared to wild type organoids. Particularly, LOX overexpression increased BMP2 and decreased BMP antagonist follistatin. Finally, we found that BMP2 treatment restored the balance of basal and differentiated cells.

Conclusions

Our data support a model whereby LOX exhibits non-canonical roles as a signaling molecule important for epithelial homeostasis in the setting of inflammation via activation of BMP pathway in esophagus. The LOX/BMP axis may be integral in esophageal epithelial differentiation and a promising target for future therapies.

Keywords

Lysyl oxidase; Organoid; BMP; Eosinophilic esophagitis

Introduction

The stratified squamous epithelium of the esophagus is the first line of protection against luminal contents including food, bacteria, and other pathogens. Epithelial barrier disruption as well as impaired epithelial differentiation are universal histologic findings in eosinophilic esophagitis (EoE), a chronic allergic disease that affects children and adults (1,2). Patients with EoE have chronic swallowing issues, vomiting, weight loss and overtime develop esophageal fibrosis and strictures. A better understanding of the perturbations that occur in the epithelial barrier of the esophagus may prevent progression of symptomatology and lifelong esophageal dysfunction.

In our previous publication, we found that lysyl oxidase (LOX), a collagen cross linking enzyme, was increased in the esophageal epithelium of patients with EoE, and to a larger degree in patients with fibrostenosis (3). LOX catalyzes extracellular collagen to form inter- and intramolecular cross-links, thus forming collagen fibers (4). LOX is a requisite for normal tissue structure and integrity with global murine deletion causing perinatal fatality due to aortic aneurysms and pulmonary abnormalities (5,6). In the setting of inflammation, enhanced cross linking within tissue has been shown to promote tissue stiffness in the context of liver fibrosis, cardiovascular disease, and breast cancer (7–9). While its role in perpetuating fibroblast activation and tissue stiffness has been described, little is known about the functional role of LOX outside of extracellular matrix remodeling and tissue stiffness.

LOX has been shown to have non-crosslinking effects in bone, skin, muscle and blood through effects on chemotaxis, gene regulation and differentiation (10–12). It has been shown to be both pro-and anti-tumorigenic, making the organ and the context particularly important in its evaluation (13). In the skin, LOX expression has been

demonstrated specifically in differentiated keratinocytes. LOX silencing inhibits keratinocyte differentiation *in vitro* and causes decreased expression of terminal differentiation markers filaggrin (FLG) and keratin 10 (KRT10) (13–15). While it seems to have a role in squamous differentiation, the function of LOX in the esophageal epithelium is unknown. LOX is upregulated in the EoE epithelium, however its role beyond collagen crosslinking in the esophagus has never been explored.

Herein, we sought to determine the role of LOX in the epithelium in the context of EoE inflammation using 3-dimensional (3D) organoid and air-liquid interface cultures. We evaluate the effect of LOX on epithelial differentiation and barrier integrity and describe a novel cytoprotective role for LOX within the inflamed esophageal epithelium.

Results

IL-13 induces LOX in the differentiated epithelium in human esophagus.

To recapitulate the EoE milieu *in vitro* and to determine the characteristics of LOX in human esophageal epithelium, we performed single-cell RNA sequencing on patient-derived organoids (PDOs) treated with interleukin (IL)-13. Three dimensional esophageal epithelial organoids allow for evaluation of the esophageal epithelial dynamics *in vitro* (16–18). Our prior work demonstrated that stimulation with IL-13, the major effector cytokine in EoE, recapitulates the epithelial reactive changes (such as basal cell hyperplasia) seen in EoE (16–18). PDOs were derived from 3 control subjects (18) and we performed single-cell RNA sequencing on each line in the presence and absence of IL-13. The integrated analysis identified 9 esophageal cell populations in the uniform manifold approximation and projection (UMAP). The 9 clusters were then categorized

into 4 groups: quiescent basal, proliferating basal, suprabasal, and superficial, based on the expression of known epithelial makers collagen type VII alpha 1 chain (*COL7A1*), dystonin (*DST*), marker of proliferation Ki-67 (*MKI67*), DNA topoisomerase II alpha (*TOP2A*), tumor protein p63 (*TP63*), involucrin (*IVL*), *FLG*, and desmoglein 1 (*DSG1*) (19,20) (Figure 1A). As expected, high *TP63* expression and low *IVL*, *FLG*, and *DSG1* expression were observed in the basal cluster. We detected *COL7A1* and *DST* transcripts in the quiescent basal, and *MKI67* and *TOP2A* transcripts in the proliferating basal cluster, respectively. In contrast, *IVL*, *FLG*, and *DSG1* were highly expressed in the differentiated cluster group (Figure 1B). We further constructed progression mapping of cell cycle phases. In agreement with expression profiling, the majority of proliferating basal populations and differentiated populations were located in G2/M and G1 cell cycle phase, respectively (Figure 1C).

Although *LOX* expression was low in nontreated samples, it was markedly upregulated by IL-13 treatment. Interestingly, cells expressing *LOX* mainly emerged in the differentiated clusters in the UMAP (Figure 1D). Pseudotime analysis was performed to determine developmental relationships between the epithelial populations in human esophagus. Inferred trajectories identified 2 unique cell fates for the quiescent cell cluster in response to IL-13 treatment: (1) toward the proliferating basal cluster and (2) toward the terminally differentiated cluster (Figure 1E). Relative expression values of *LOX* were plotted along pseudotime axis (Figure 1F). The increased expression of *LOX* at the late pseudotime suggests that IL-13 upregulates LOX in differentiated populations within human esophageal epithelium. We further focused on heterogeneity of LOX expressing cells in the differentiated clusters (Figure 1D). Only 10% of the superficial cells were expressing LOX in IL-13-stimulated PDOs. To reveal features of the LOX expressing

cells, we performed differentially expression gene (DEG) analysis between LOX expressing (LOX^+) cells and LOX non-expressing (LOX^-) cells in the IL-13-treated superficial population. Expression patterns of the top 10 upregulated and downregulated DEGs are shown in Figure 1G. The most highly DEG in the LOX^+ cells compared to the LOX^- cells was keratin 1, followed by keratin 13, and KRT10 which are known as a differentiation marker. Gene Ontology analysis using DEGs demonstrated that heterogeneity of the LOX^+ and LOX^- cells was related to regulation of cell migration, squamous cell differentiation, and cytoskeleton in IL-13-stimulated PDOs (Figure 1H).

LOX promotes cell differentiation in esophageal epithelium.

To investigate the impact of induced LOX in the esophageal epithelium, we overexpressed LOX in the immortalized nontransformed normal human esophageal epithelial cell line (EPC2-hTERT) (3,17,18,21). Green fluorescent protein-transduced (GFP) cells were used as a control. Quantitative reverse transcription-polymerase chain reaction (qRT-PCR) and immunoblotting confirmed increased expression in LOX overexpressing EPC2-hTERT (LOX OE) cells compared to GFP cells in monolayer culture (Figure 2A and 2B).

We next evaluated 3D organoid cultures (16,17) stimulated with IL-13 (22,23). Ectopic LOX expression resulted in decreased expression of basal cell marker genes SRY-box transcription factor 2 (*SOX2*), keratin 14 (*KRT14*), and *TP63*, and increased expression of differentiation marker genes *IVL*, *FLG*, and loricrin (*LOR*), in both nontreated and IL-13-treated organoids (Figure 2C). We also assessed organoid morphology. Hematoxylin and eosin stain (H&E) staining revealed that LOX OE organoids had advanced inner core hyperkeratosis compared to GFP organoids. IL-13-

204 treated GFP organoids had expansion of the basal cell population, as seen in EoE (1),
205 with thickening of the outer basaloid layer. However, this effect was attenuated in IL-13-
206 treated LOX OE organoids (Figure 2D). Immunohistochemistry and immunofluorescence
207 staining demonstrated elevation of TP63 and depression of IVL and FLG levels by IL-13
208 in GFP organoids. On the other hand, LOX OE organoids demonstrated reduced
209 expression of TP63 and enhanced expression of IVL and FLG in both untreated and IL-
210 13 conditions compared to GFP organoids (Figure 2D). These findings support the
211 conclusion that LOX partially mitigates the disrupted cellular gradient caused by IL-13
212 stimulus.

213 Since only basaloid cells (and not terminally differentiated cells) are capable of
214 forming organoids, we assessed organoid formation rate (OFR) to confirm whether LOX
215 OE cell has reduced OFR due to enhanced differentiation. Although OFR did not
216 significantly change after seeding from 2D basaloid-monolayers into organoids (P0), it
217 was significantly decreased in passaged LOX OE organoids (P1), suggesting that LOX
218 OE organoids comprise more differentiated cells than GFP organoids (Figure 3A and 3B).
219 Taken together, these results confirm that overexpressing LOX promotes epithelial
220 differentiation.

221

222 ***LOX improves barrier integrity in esophageal epithelium.***

223 Disturbed squamous cell differentiation alters epithelial barrier integrity (24,25).
224 This disruption is crucial in the pathogenesis of EoE (26–28). Thus, we sought to
225 elucidate if LOX is implicated in barrier regulation. DSG1 and desmocollin-1 (DSC1),
226 members of the desmosomal cadherin family, are required for adhesive intercellular
227 junctions and maintenance of epithelial homeostasis (29,30). Interestingly, while IL-13

228 treatment decreased transcript levels of *DSG1* and *DSC1* in organoids, LOX
229 overexpression increased their expression at baseline and partially rescued the effect of
230 IL-13 (Figure 4A).

231 To directly assess the effect of LOX on barrier function, we used the ALI system
232 which mimics an *in vivo* epithelial environment and measured transepithelial electrical
233 resistance (TEER) (31) (Figure 4B). IL-13 treatment increased barrier permeability in the
234 epithelium as measured by TEER. Conversely, LOX overexpression improved the IL-13-
235 induced barrier deficiency by 1.4-fold compared to GFP cells (Figure 4C). H&E staining
236 of GFP cultures also showed impaired squamous stratification in response to IL-13.
237 However, LOX overexpression counteracted the disruption caused by IL-13. We
238 performed staining for TP63, IVL, FLG, and DSG1 in ALI cultures. As seen in organoids,
239 although IL-13 stimulation prevented differentiation and barrier-related protein
240 expression in the epithelium, LOX overexpression enhanced IVL, FLG and DSG1 in both
241 untreated and IL-13 stimulated cultures. Collectively, these data show that LOX promotes
242 normal cell differentiation and supports epithelial integrity including in the setting of IL-
243 13 stimulation.
244
245 ***Transcriptome profiling reveals pathways associated with LOX expression in***
246 ***esophageal epithelium.***
247 To understand the mechanism by which LOX regulates epithelial integrity, we
248 performed RNA sequencing on LOX OE organoids. DEG analysis using DESeq2 (32)
249 identified 2446 upregulated ($P < 0.05$ and $\log_2$(fold change) ≥ 0.585) and 2923
250 downregulated ($P < 0.05$ and $\log_2$(fold change) ≤ -0.585) genes in LOX OE organoids
251 compared to GFP organoids (Figure 5A and 5B). Gene Ontology analysis of DEGs

252 revealed that cell differentiation and keratinization-related terms were enriched in LOX
253 OE organoids (Figure 5C). By contrast, cell proliferation-related terms were decreased
254 (Figure 5D). Furthermore, Gene Set Enrichment Analysis (GSEA) on the Pathway
255 Interaction Database (PID) (33) revealed that gene signatures associated with bone
256 morphogenetic protein (BMP), transforming growth factor-β (TGFβ), and WNT
257 pathways, were significantly enriched in LOX OE organoids (false discovery rate; FDR
258 < 0.25; Figure 5E). These results are consistent with our previous results showing a role
259 for LOX in modulating esophageal epithelial differentiation.
260
261 ***BMP signaling pathway is activated in LOX overexpressing organoids.***
262 Recent studies demonstrated that BMP pathway is essential for esophageal
263 progenitor cell differentiation and disrupted BMP signaling results in basal cell
264 hyperplasia in EoE (34,35). Therefore, we postulated that BMP signaling pathway could
265 be integral in LOX-supported differentiation (Figure 6A). We investigated BMP ligands
266 and BMP receptors (BMPRs) from the PID gene sets presented in Figure 5E and 6A.
267 *BMP2*, *BMP6*, *BMPR1B*, and *BMPR2* were significantly elevated in LOX OE organoids
268 compared to GFP organoids (by 2.5-fold, 18.3-fold, 4.8-fold, and 1.2-fold, respectively).
269 Intriguingly, we found that the BMP antagonist follistatin (*FST*) was significantly
270 decreased by 0.36-fold in LOX OE organoids (Figure 6B).
271 We validated these findings by qRT-PCR, western blot, and
272 immunohistochemistry in the setting of IL-13 stimulation (Figure 6C-F). Transcript levels
273 of *BMP2* were increased by 4.0-fold and 3.2-fold in untreated and IL-13-stimulated LOX
274 OE organoids compared to GFP organoids, respectively. IL-13 stimulus led to increased
275 expression of *FST* in GFP organoids, while LOX overexpression reduced this effect by

0.62-fold and 0.21-fold in untreated and IL-13-stimulated LOX OE organoids, respectively (Figure 6C). Protein levels of BMP2 and downstream transcription factor phospho-SMAD1/5/9 (p-SMAD1/5/9) were also increased in LOX OE organoids (Figure 6D). FST, which was robustly expressed in IL-13 stimulated organoids, was decreased in the setting of LOX overexpression (Figure 6E and 6F). These data support a model in which overexpression of LOX inhibits FST leading to increased BMP signaling.

BMP2 promotes cell differentiation in esophageal epithelium.

Finally, we investigated whether BMP2 is involved in esophageal epithelial differentiation and barrier integrity. Treatment with recombinant BMP2 led to decreased *TP63* mRNA expression and increased *IVL*, *FLG*, *DSG1*, and *DSC1* mRNA expression in monolayer-cultured EPC2-hTERT cell (Figure 7A). Immunoblotting demonstrated similar results with increased p-SMAD1/5/9, IVL, and DSG1 in BMP2-treated cells (Figure 7B). Consistent with the results in monolayer culture, BMP2-treated organoids showed decreased expression of basal genes (SOX2 and TP63) and increased expression of differentiation and junctional protein genes (IVL, FLG, LOR, DSG1, and DSC1) (Figure 7C and 7D). BMP2 treatment also reduced organoid formation capacity, further supporting the notion that BMP2 enhances differentiation and reduces the basal population (Figure 7E). In summary, our findings suggest that LOX has a protective role in the esophageal epithelium in which it acts to restore homeostasis in EoE via activation of BMP signaling.

Discussion

Lysyl oxidase is an extracellular matrix remodeling enzyme, which acts to cross link collagen thereby enhancing tissue stiffness. LOX is expressed in the epithelium of the prostate, retina, and skin as well as other locations (36–38), however its role in the esophageal epithelium in homeostasis and disease is unknown. Herein, we describe a non-canonical role for LOX in the esophageal epithelium and a potential protective role in epithelial differentiation and barrier integrity. Building upon our previous work demonstrating that LOX was upregulated in the EoE epithelium, we now show that LOX is expressed in the differentiated esophageal epithelium where it has non-collagen-crosslinking roles. LOX overexpression models demonstrate enhanced differentiation and barrier integrity even in the setting of IL-13 stimulation in the esophageal epithelium. Utilizing unbiased transcriptomic approaches, we found that the BMP pathway was enriched in LOX OE cells and that LOX OE cells have increased expression of BMP2, while BMP antagonist follistatin is decreased. This effect is maintained despite IL-13 stimulation. These results help to elucidate the contribution of LOX-supported differentiation and barrier integrity both in homeostasis and in the context of allergic insult.

Epithelial changes in EoE disrupt the mucosal barrier which normally provides protection from acid and food particles during normal swallows. Current treatment strategies are aimed at decreasing the invasion of inflammatory cells into the esophagus. However, we have found that epithelial changes persist even in patients in remission with low eosinophil counts (2). Thus, determining mechanisms to restore homeostasis to the esophageal epithelium represents an unexplored avenue of research with therapeutic potential. We now highlight a novel role for LOX in restoration of epithelial homeostasis. LOX silencing has been shown to impair keratinocyte differentiation of the skin (36). In

fact, *in vitro* skin models show that LOX expression is increased in early differentiation and knockdown inhibits terminal differentiation. Taken together, these results suggest that increased LOX in the setting of inflammation may serve to re-establish differentiation and barrier during injury in the squamous mucosa.

Fibrosis is a major complication in EoE, and since LOX is a collagen crosslinker, it would be tempting to use LOX inhibitors to prevent fibrosis. However, our data demonstrating the protective roles of LOX in the esophageal epithelium in the context of Th2 inflammation would suggest that global LOX inhibition would have detrimental effects on the epithelial barrier. It would therefore be advantageous to target the crosslinker activity of LOX without effecting its non-crosslinking functions or vice versa. In that regard, our identification of the beneficial role of the LOX/BMP axis in the esophageal epithelium may represent a new approach to mitigating EoE, which could be employed via a topical approach. Topical steroid preparations are often employed in EoE to spare the negative consequences of systemic treatment with steroids (39,40). Furthermore, recombinant human BMP2 is currently approved by the Food and Drug Administration to promote bone healing in orthopedics (41–43). Building off of this and our *in vitro* findings of the protective role of BMP2 in the setting of IL-13 stimulation (Figure 7), it may be possible to employ preparations of BMP2 agonists to enhance esophageal epithelial barrier integrity.

BMP2, a member of the TGFβ superfamily, is essential for embryogenesis and development of the gut, and the BMP pathway affects morphogenesis of esophageal epithelial progenitor cells (44–47). We revealed that overexpression of LOX results in increased expression of BMP2 and increased squamous differentiation in esophageal organoids. Interestingly, downregulated BMP2 expression by fibroblast growth factor 9,

348 which is upregulated in patients with EoE, has been proposed as the mechanism of
349 hyperplasia in EoE (48). Furthermore, basal cell hyperplasia in the EoE epithelium,
350 specifically in the setting of IL-13 stimulation, is associated with inhibition of the BMP
351 pathway in human disease and murine models (34). Herein, we demonstrate the role of
352 LOX specifically in differentiated cells to maintain barrier integrity and restore
353 homeostasis. Future work will interrogate the mechanism by which LOX activates the
354 BMP pathway to exert these protective roles. One possibility is downregulation of the
355 BMP antagonist follistatin (49) by LOX. We demonstrated decreased follistatin levels in
356 LOX OE organoids, even in the setting of IL-13 stimulation (Figure 6). Interestingly, IL-
357 13/STAT6 pathway directly upregulates follistatin, and its increased levels have been
358 reported in EoE patients and murine models (34). Correspondingly, knockdown of
359 follistatin accelerates epithelial differentiation in esophageal cells. To date, although
360 reactive oxidative stress has been shown to mediate the differentiation by the activated
361 BMP in EoE (34), the specific mechanism remains to be elucidated.

362 One weakness of this study is that we rely on cell culture techniques as there is no
363 *in vivo* model of LOX overexpression. LOX knock out mouse models would complement
364 this work, however, these models are embryonic lethal and tissue specific knock out
365 mouse strains do not exist. To contend with these limitations, we utilize 3D cultures
366 (organoid and ALI culture) to replicate the proliferation and renewal patterns *in vitro*.
367 Another potential weakness is that while LOX is upregulated in EoE, our model may be
368 inducing higher overexpression levels than observed *in vivo*. However, the benefit of this
369 model is that it allows for evaluation of the mechanistic effects of LOX without the
370 secondary effects of inflammatory cytokines.

371 The esophageal epithelial barrier is maintained by an exquisitely regulated

proliferation and differentiation gradient. The perturbations lead to symptoms as well as inflammation. Herein, we describe a novel role for LOX involving maintenance of differentiation and barrier integrity independent of its effects in subepithelial matrix remodeling. Epithelial LOX may serve to re-establish homeostasis in the setting of inflammation via BMP activation, underscoring the diverse functions of LOX in the esophagus. Investigation of the LOX-BMP pathway may provide novel insights into the pathogenesis and be a promising therapeutic approach for EoE. Further, elucidating these mechanisms may have implications for epithelial disruption in disorders beyond EoE, including caustic ingestions and gastroesophageal reflux disease.

Methods

Cell line and monolayer culture

EPC2-hTERT cells were cultured in keratinocyte-serum free medium with 0.09 mM Ca^{2+} (KSFM; Thermo Fisher Scientific Inc., Waltham, MA, USA) supplemented with bovine pituitary extract (50 μg/ml), human recombinant epidermal growth factor (1 ng/ml), and 1% penicillin-streptomycin. The cells were incubated at 37°C in a 5% humidified CO_2 atmosphere (50,51).

3-dimensional esophageal organoid culture

EPC2-hTERT organoids were cultured as described previously (16–18). Briefly, EPC2-hTERT cells were dissociated into a single cell suspension and placed into Matrigel basement membrane matrix (Corning Inc., Corning, NY, USA) under KSFM modified with 0.6 mM Ca^{2+}. Organoids were grown for 7 days, followed by treatment with 10

ng/ml IL-13, 10 ng/ml recombinant BMP2 protein (R&D Systems, Inc., Minneapolis, MN, USA), or vehicle (phosphate-buffered saline for IL-13 and hydrochloride for BMP2) for 4 days. We then used the day 11 organoids for further analyses. OFR was defined as the number of organoids ≥ 50 μm divided by the total seeded cells in each well (17,18).

Air-liquid interface culture

EPC2-hTERT cells were seeded on transwell permeable supports with 0.4 μm pore (3470; Corning) and grown with KSMF (0.09 mM Ca^{2+}) for initial 3 days to confluency. Cultures were then switched to high-calcium KSFM (1.8 mM Ca^{2+}) for 5 days. The media was removed from the apical compartment on day 8 to induce epithelial differentiation and stratification. 10 μg/ml IL-13 (or vehicle) was applied in the basolateral compartment from day 9 to 14. In order to assess epithelial barrier integrity, TEER was measured with Epithelial Volt/Ohm (TEER) Meter (World Precision Instruments, Sarasota, FL, USA). The day 14 ALI-cultured epithelium was used for TEER measurement and histology.

Bioinformatic analysis of single-cell RNA sequencing data

PDOs were stimulated with vehicle or IL-13 (10 μg/ml) from day 7 to day 11 and the day 11 PDOs were then dissociated into a single cell suspension for single-cell RNA sequencing (18). Dead Cell Removal Kit (Miltenyi Biotec, Bergisch Gladbach, Germany) was used to guarantee cell viability. The raw count matrix with barcode and feature information for each sample were imported and transformed to Seurat (version 4.2.0) objects for further processing. Genes expressed in 3 or fewer cells were excluded from analysis. To eliminate dead cells or doublets, cells with the expression of less than 700 or over 6000 genes, respectively, were excluded. Additionally, cells with over 10% of their

transcripts consisting of mitochondrial genes were excluded. Seurat integration workflow was used to integrate the top 3000 variable genes, as anchors, across cells for control samples (52). After integration, dimensionality reduction used the genes and values that were pre-processed using the integration workflow. Principal component analysis was used for initial dimensionality reduction and later for clustering, resulting in 20 principal components. The components were then used as input to the UMAP dimensionality reduction procedure using 20 neighbors for local neighborhood approximation and embedding into 2 components for visualization. Clustering was initialized with a Shared Nearest Neighbor (SNN) graph by first determining 20 nearest neighbors for each cell, and then determined by a modularity optimization algorithm by Waltman and van Eck (53). Cell type annotations for each cluster are based on the expression of marker genes and DEGs. To better compare the IL-13 treated samples to the control data, IL-13 data were projected to control data after filtering and integration using Seurat projection/query workflow. For DEG analysis on the IL-13 treated PDOs, cells with a LOX expression greater than 0 were defined as LOX^+ cells and cells with a LOX expression of 0 were defined as LOX^- cells in the superficial cluster.

Trajectory analysis

Monocle 3 (version 1.0.0) was used to infer the trajectory analysis based on the single-cell RNA sequencing data. Seurat objects from upstream analysis were converted to Monocle objects, and then reversed graph embedding was applied to yield principal graph that is allowed to branch from the reduced dimension space (54). Pseudotime trajectory are defined and derived by selecting the specific cells as roots based on the prior knowledge of the cell type.

444

445 ***Bulk mRNA sequencing and gene expression analysis***

446 GFP and LOX OE organoids were grown for 11 days and then harvested for RNA
447 sequencing. Sequencing libraries were constructed from total RNA (1 μg) using a TruSeq
448 Stranded mRNA Library Prep (Illumina Inc., San Diego, CA, USA). RNA sequencing
449 was performed on Illumina HiSeq2000 platform. We used kallisto (55) and human
450 reference genome hg38 for alignment. Mapped reads were analyzed with DESeq2 (32).
451 DEGs were determined as $P < 0.05$ and $\log_2$(fold change) ≥ 0.585 or ≤ -0.585. Using
452 DEGs, Gene Ontology enrichment analysis was provided by topGO package (56). Top 5
453 enriched or depleted terms with the lowest FDR values in LOX OE organoids were
454 selected. The 'stat' output field from DESeq2 was then used as input for GSEA (57,58)
455 preranked analysis to identify enriched pathways from the PID.

456

457 ***Lentivirus-mediated gene transfer***

458 Lentiviral vectors pLX304-eGFP and pLX304-LOX were constructed by Gateway LR
459 reaction of entry clones pENTR223-LOX (HsCD00378945, PlasmID Harvard Medical
460 School) and pDONR221-eGFP (Addgene vector 25899) with destination vector pLX304
461 (Addgene vector 25890). VSV-g coated lentiviral particles were prepared by transfecting
462 293T cells with 9 μg of psPAX, 0.9 μg of pMD2.G, and 9 μg of overexpression vector
463 using Lipofectamine 2000 Transfection Reagent (Thermo Fisher Scientific Inc.). EPC2-
464 hTERT cells were transduced by spinfection and selected with 10 μg/ml blasticidin (59).

465

466 ***Quantitative reverse transcription-polymerase chain reaction***

467 RNA extraction and reverse transcription were carried out as described previously

(21,51). Real-time qRT-PCR was performed with TaqMan Gene Expression Assays (Thermo Fisher Scientific Inc.) for *LOX* (Hs00942480_m1), *SOX2* (Hs01053049_s1), *KRT14* (Hs03044364_m1), *TP63* (Hs00978340_m1), *IVL* (Hs00846307_s1), *FLG* (Hs00856927_g1), *LOR* (Hs01894962_s1), *BMP2* (Hs00154192_m1), *FST* (Hs01121165_g1), and glyceraldehyde-3-phosphate dehydrogenase (*GAPDH*; Hs02786624_g1) using the StepOnePlus Real-Time PCR System (Thermo Fisher Scientific Inc.). Relative mRNA levels of each gene were normalized to *GAPDH* levels as a housekeeping control.

Western Blot

Whole-cell lysates from cells in monolayer culture and 3D organoids were prepared as described previously (17). Equivalent amounts (20-40 μg) of protein were loaded into a NuPAGE 4 to 12% Bis-Tris gel. Following electrophoresis, transfer to a polyvinylidene difluoride membrane, and blocking with 5% bovine serum albumin or non-fat milk, membranes were incubated with primary antibodies at 4°C overnight. The primary antibodies used were follows: anti-LOX (1:500; NB100-2527; Novus Biologicals, Centennial, CO, USA), anti-TP63 (1:1000; ab124762; Abcam, Cambridge, UK), anti-IVL (1:1000; I9018; Millipore Sigma, Burlington, MA, USA), anti-DSG1 (1:1000; sc-137164; Santa Cruz Biotechnology, Dallas, TX, USA), anti-BMP2 (1:1000; ab214821; Abcam), anti-phospho-SMAD1/5/9 (1:1000;13820S; Cell Signaling Technology, Danvers, MA, USA), and anti-β-actin (1:5000; A5316; Millipore Sigma). Immunoblots were detected with an appropriate horseradish peroxidase (HRP)-conjugated secondary antibody (1:2000; NA934 or NA 931; Amersham BioSciences, Buckinghamshire, UK) by ECL detection (Bio-Rad Laboratories, Hercules, CA, USA). β-Actin served as a

492 loading control.

493

494 ***Immunohistochemistry and immunofluorescence***

495 Organoids were fixed and embedded as described previously (16,17), and subjected to
496 hematoxylin and eosin staining, immunohistochemistry, and immunofluorescence.
497 For immunohistochemistry, after deparaffinization and rehydration, antigens were
498 retrieval by high-pressure cooking, Following, peroxidase quenching and blocking with
499 an appropriate serum (Jackson ImmunoResearch), sections were incubated with primary
500 anti-TP63 monoclonal antibody (1:1000; ab124762; Abcam) and anti-follistatin
501 monoclonal antibody (1:50; MAB669; R&D Systems, Inc.) at 4°C overnight and then
502 with an appropriate biotinylated secondary antibody (1:200; Vector Laboratories,
503 Burlingame, CA, USA). The signal was detected with VECTASTAIN Elite ABC-HRP
504 Kit (PK-6100; Vector Laboratories). DAB Substrate Kit (SK-4100; Vector Laboratories)
505 was used for color reaction. For follistatin staining, slides were quantified with following
506 score: 1 is negative to weak, 2 is weak to moderate, 3 is moderate to strong, and 4 is
507 strong staining. Ten organoids per condition were used for the evaluation.
508 For immunofluorescence, sections were stained with primary anti-IVL monoclonal
509 antibody (1:100, I9018; Millipore Sigma), anti-FLG monoclonal antibody (1:100; MA5-
510 13440; Thermo Fisher Scientific Inc.), and anti-DSG1 monoclonal antibody (1:100; sc-
511 137164; Santa Cruz Biotechnology) at 4°C overnight and then with Cy2 or Cy5-
512 AffiniPure Donkey Anti-Mouse IgG (H+L) secondary antibody (1:500; 715-225-150 or
513 715-175-150; Jackson ImmunoResearch, West Grove, PA, USA) at room temperature for
514 1 h. Nuclei were stained with 4′,6-diamidino-2-phenylindole (DAPI; 17985-50; Electron
515 Microscopy Sciences, Hatfield, PA, USA). Images were taken with an All-in-One

Fluorescence Microscope BZ-X710 (KEYENCE Corp., Osaka, Japan). The images were evaluated in 5 different locations in high-power field per condition, and representatives are shown.

Statistical analysis

Data are presented as means ± standard deviations (SDs). Continuous variables were analyzed by two-tailed Student's t-test for two independent groups or analysis of variance for multigroup. All statistical analyses were conducted with GraphPad Prism (GraphPad Software, San Diego, CA, USA). A *P* value of less than 0.05 was considered statistically significant.

All authors had access to the study data and had reviewed and approved the final manuscript.

Study approval

Not applicable.

Acknowledgments

We thank to the Molecular Pathology and Imaging Core (Kate Bennett, Rebecca Ly, and Jonathan P Katz) for technical support. Schematics were created with BioRender.com.

References

1. Muir A, Falk GW. Eosinophilic Esophagitis: A Review. Journal of the American Medical Association 2021;326:1310–8.
2. Whelan KA, Godwin BC, Wilkins B, Elci OU, Benitez A, DeMarshall M, Sharma M, Gross J, Klein-Szanto AJ, Liacouras CA, Dellon ES, Spergel JM, Falk GW, Muir AB, Nakagawa H.

Persistent Basal Cell Hyperplasia Is Associated With Clinical and Endoscopic Findings in Patients With Histologically Inactive Eosinophilic Esophagitis. Clinical Gastroenterology and Hepatology 2020;18:1475–82.

3. Kasagi Y, Dods K, Wang JX, Chandramouleeswaran PM, Benitez AJ, Gambanga F, Kluger J, Ashorobi T, Gross J, Tobias JW, Klein-Szanto AJ, Spergel JM, Cianferoni A, Falk GW, Whelan KA, Nakagawa H, Muir AB. Fibrostenotic eosinophilic esophagitis might reflect epithelial lysyl oxidase induction by fibroblast-derived TNF-α. Journal of Allergy and Clinical Immunology 2019;144:171–82.
4. Chen W, Yang A, Jia J, Popov YV, Schuppan D, You H. Lysyl Oxidase (LOX) Family Members: Rationale and Their Potential as Therapeutic Targets for Liver Fibrosis. Hepatology 2020;72:729–41.
5. Mäki JM, Räsänen J, Tikkanen H, Sormunen R, Mäkikallio K, Kivirikko KI, Soininen R. Inactivation of the lysyl oxidase gene Lox leads to aortic aneurysms, cardiovascular dysfunction, and perinatal death in mice. Circulation 2002;106:2503–9.
6. Mäki JM, Sormunen R, Lippo S, Kaarteenaho-Wiik R, Soininen R, Myllyharju J. Lysyl oxidase is essential for normal development and function of the respiratory system and for the integrity of elastic and collagen fibers in various tissues. American Journal of Pathology 2005;167:927–36.
7. Maller O, Drain AP, Barrett AS, Borgquist S, Ruffell B, Zakharevich I, Pham TT, Gruosso T, Kuasne H, Lakins JN, Acerbi I, Barnes JM, Nemkov T, Chauhan A, Gruenberg J, Nasir A, Bjarnadottir O, Werb Z, Kabos P, Chen YY, Hwang ES, Park M, Coussens LM, Nelson AC, Hansen KC, Weaver VM. Tumour-associated macrophages drive stromal cell-dependent collagen crosslinking and stiffening to promote breast cancer aggression. Nature Materials 2021;20:548–59.
8. von Kleeck R, Roberts E, Castagnino P, Bruun K, Brankovic SA, Hawthorne EA, Xu T, Tobias JW, Assoian RK. Arterial stiffness and cardiac dysfunction in Hutchinson-Gilford Progeria syndrome corrected by inhibition of lysyl oxidase. Life Science Alliance 2021;4:e202000997.
9. Perepelyuk M, Terajima M, Wang AY, Georges PC, Janmey PA, Yamauchi M, Wells RG. Hepatic stellate cells and portal fibroblasts are the major cellular sources of collagens and lysyl oxidases in normal liver and early after injury. American Journal of Physiology – Gastrointestinal and Liver Physiology 2013;304:605–14.
10. Trackman PC. Enzymatic and non-enzymatic functions of the lysyl oxidase family in bone. Matrix Biology 2016;52-54:7–18.
11. Lucero HA, Ravid K, Grimsby JL, Rich CB, DiCamillo SJ, Mäki JM, Myllyharju J, Kagan HM. Lysyl oxidase oxidizes cell membrane proteins and enhances the chemotactic response of vascular smooth muscle cells. Journal of Biological Chemistry 2008;283:24103–17.
12. Laczko R, Csiszar K. Lysyl oxidase (Lox): Functional contributions to signaling pathways. Biomolecules 2020;10:1093.
13. Bouez C, Reynaud C, Noblesse E, Thépot A, Gleyzal C, Kanitakis J, Perrier E, Damour O, Sommer P. The lysyl oxidase LOX is absent in basal and squamous cell carcinomas and its knockdown induces an invading phenotype in a skin equivalent model. Clinical Cancer Research 2006;12:1463–9.
14. Le Provost GS, Debret R, Cenizo V, Aimond G, Pez F, Kaniewski B, André V, Sommer P. Lysyl oxidase silencing impairs keratinocyte differentiation in a reconstructed-epidermis model. Experimental Dermatology 2010;19:1080–7.
15. Noblesse E, Cenizo V, Bouez C, Borel A, Gleyzal C, Peyrol S, Jacob MP, Sommer P, Damour O. Lysyl oxidase-like and lysyl oxidase are present in the dermis and epidermis of a skin equivalent and in human skin and are associated to elastic fibers. Journal of Investigative Dermatology 2004;122:621–30.
16. Nakagawa H, Kasagi Y, Karakasheva TA, Hara T, Aaron B, Shimonosono M, Kijima T, Giroux V, Bailey D, Wilkins B, Abrams JA, Falk GW, Aceves SS, Spergel JM, Hamilton KE, Whelan KA, Muir AB. Modeling Epithelial Homeostasis and Reactive Epithelial Changes in Human and Murine Three-Dimensional Esophageal Organoids. Current Protocols in Ste Cell Biology 2020;52:e106.

17. Kasagi Y, Chandramouleeswaran PM, Whelan KA, Tanaka K, Giroux V, Sharma M, Wang J, Benitez AJ, DeMarshall M, Tobias JW, Hamilton KE, Falk GW, Spergel JM, Klein-Szanto AJ, Rustgi AK, Muir AB, Nakagawa H. The Esophageal Organoid System Reveals Functional Interplay Between Notch and Cytokines in Reactive Epithelial Changes. Cellular and Molecular Gastroenterology and Hepatology 2018;5:333–52.
18. Hara T, Kasagi Y, Wang J, Sasaki M, Aaron B, Karami A, Shimonosono M, Shimonosono R, Maekawa H, Dolinsky L, Wilkins B, Klein J, Wei J, Nunes K, Lynch K, Spergel JM, Hamilton KE, Ruffner MA, Karakasheva TA, Whelan KA, Nakagawa H, Muir AB. CD73 + epithelial progenitor cells which contribute to homeostasis and renewal are depleted in eosinophilic esophagitis. Cellular and Molecular Gastroenterology and Hepatology 2022;13:1449–67.
19. Busslinger GA, Weusten BLA, Bogte A, Begthel H, Brosens LAA, Clevers H. Human gastrointestinal epithelia of the esophagus, stomach, and duodenum resolved at single-cell resolution. Cell Reports 2021;34:108819.
20. Rochman M, Wen T, Kotliar M, Dexheimer PJ, Ben-Baruch Morgenstern N, Caldwell JM, Lim HW, Rothenberg ME. Single-cell RNA-Seq of human esophageal epithelium in homeostasis and allergic inflammation. JCI Insight 2022;7:e159093.
21. Muir AB, Lim DM, Benitez AJ, Modayur Chandramouleeswaran P, Lee AJ, Ruchelli ED, Spergel JM, Wang ML. Esophageal epithelial and mesenchymal cross-talk leads to features of epithelial to mesenchymal transition in vitro. Experimental Cell Research 2013;319:850–9.
22. Blanchard C, Wang N, Stringer KF, Mishra A, Fulkerson PC, Abonia JP, Jameson SC, Kirby C, Konikoff MR, Collins MH, Cohen MB, Akers R, Hogan SP, Assa'ad AH, Putnam PE, Aronow BJ, Rothenberg ME. Eotaxin-3 and a uniquely conserved gene-expression profile in eosinophilic esophagitis. Journal of Clinical Investigation 2006;116:536–47.
23. Blanchard C, Stucke EM, Rodriguez-Jimenez B, Burwinkel K, Collins MH, Ahrens A, Alexander ES, Butz BK, Jameson SC, Kaul A, Franciosi JP, Kushner JP, Putnam PE, Abonia JP, Rothenberg ME. A striking local esophageal cytokine expression profile in eosinophilic esophagitis. Journal of Allergy and Clinical Immunology. 2011;127:208–17.
24. Wu L, Oshima T, Li M, Tomita T, Fukui H, Watari J, Miwa H. Filaggrin and tight junction proteins are crucial for IL-13-mediated esophageal barrier dysfunction. American Journal of Physiology – Gastrointestinal and Liver Physiology 2018;315:341–50.
25. Rochman M, Travers J, Miracle CE, Bedard MC, Wen T, Azouz NP, Caldwell JM, Kc K, Sherrill JD, Davis BP, Rymer JK, Kaufman KM, Aronow BJ, Rothenberg ME. Profound loss of esophageal tissue differentiation in patients with eosinophilic esophagitis. Journal of Allergy and Clinical Immunology 2017;140:738–49.
26. Sherrill JD, Kc K, Wu D, Djukic Z, Caldwell JM, Stucke EM, Kemme KA, Costello MS, Mingler MK, Blanchard C, Collins MH, Abonia JP, Putnam PE, Dellon ES, Orlando RC, Hogan SP, Rothenberg ME. Desmoglein-1 regulates esophageal epithelial barrier function and immune responses in eosinophilic esophagitis. Mucosal Immunology 2014;7:718–29.
27. Katzka DA, Tadi R, Smyrk TC, Katarya E, Sharma A, Geno DM, Camilleri M, Iyer PG, Alexander JA, Buttar NS. Effects of topical steroids on tight junction proteins and spongiosis in esophageal epithelia of patients with eosinophilic esophagitis. Clinical Gastroenterology and Hepatology 2014;12:1824–9.
28. Katzka DA, Ravi K, Geno DM, Smyrk TC, Iyer PG, Alexander JA, Mabary JE, Camilleri M, Vaezi MF. Endoscopic mucosal impedance measurements correlate with eosinophilia and dilation of intercellular spaces in patients with eosinophilic esophagitis. Clinical Gastroenterology and Hepatology 2015;13:1242–8.
29. Simpson CL, Patel DM, Green KJ. Deconstructing the skin: cytoarchitectural determinants of epidermal morphogenesis. Nature Reviews Molecular Cell Biology 2011;12:565–80.
30. Sherrill JD, Kc K, Wu D, Djukic Z, Caldwell JM, Stucke EM, Kemme KA, Costello MS, Mingler MK, Blanchard C, Collins MH, Abonia JP, Putnam PE, Dellon ES, Orlando RC, Hogan SP, Rothenberg ME. Desmoglein-1 regulates esophageal epithelial barrier function and immune responses in eosinophilic esophagitis. Mucosal Immunology 2014;7:718–29.
31. Ruffner MA, Song L, Maurer K, Shi L, Carroll MC, Wang JX, Muir AB, Spergel JM, Sullivan KE. Toll-like receptor 2 stimulation augments esophageal barrier integrity. Allergy

2019;74:2449–60.
32. Love MI, Huber W, Anders S. Moderated estimation of fold change and dispersion for RNA-seq data with DESeq2. Genome Biology 2014;15:550.
33. Schaefer CF, Anthony K, Krupa S, Buchoff J, Day M, Hannay T, Buetow KH. PID: the Pathway Interaction Database. Nucleic Acids Research 2009;37:D674–9.
34. Jiang M, Ku WY, Zhou Z, Dellon ES, Falk GW, Nakagawa H, Wang ML, Liu K, Wang J, Katzka DA, Peters JH, Lan X, Que J. BMP-driven NRF2 activation in esophageal basal cell differentiation and eosinophilic esophagitis. Journal of Clinical Investigation 2015;125:1557–68.
35. Zhang Y, Yang Y, Jiang M, Huang SX, Zhang W, Al Alam D, Danopoulos S, Mori M, Chen YW, Balasubramanian R, Chuva de Sousa Lopes SM, Serra C, Bialecka M, Kim E, Lin S, Toste de Carvalho ALR, Riccio PN, Cardoso WV, Zhang X, Snoeck HW, Que J. 3D Modeling of Esophageal Development using Human PSC-Derived Basal Progenitors Reveals a Critical Role for Notch Signaling. Cell Stem Cell 2018;23:516–29.
36. Le Provost GS, Debret R, Cenizo V, Aimond G, Pez F, Kaniewski B, André V, Sommer P. Lysyl oxidase silencing impairs keratinocyte differentiation in a reconstructed-epidermis model. Experimental Dermatology 2010;19:1080–7.
37. Omori K, Fujiseki Y, Omori K, Suzukawa J, Inagaki C. Regulation of the expression of lysyl oxidase mRNA in cultured rabbit retinal pigment epithelium cells. Matrix Biology 2002;21:337–48.
38. Nilsson M, Hägglöf C, Hammarsten P, Thysell E, Stattin P, Egevad L, Granfors T, Jernberg E, Wikstrom P, Halin Bergström S, Bergh A. High Lysyl Oxidase (LOX) in the Non-Malignant Prostate Epithelium Predicts a Poor Outcome in Prostate Cancer Patient Managed by Watchful Waiting. PLoS One 2015;10:e0140985.
39. Gupta SK, Vitanza JM, Collins MH. Efficacy and safety of oral budesonide suspension in pediatric patients with eosinophilic esophagitis. Clinical Gastroenterology and Hepatology 2015;13:66–76.
40. Straumann A, Conus S, Degen L, Frei C, Bussmann C, Beglinger C, Schoepfer A, Simon HU. Long-term budesonide maintenance treatment is partially effective for patients with eosinophilic esophagitis. Clinical Gastroenterology and Hepatology 2011;9:400–9.
41. Wang RN, Green J, Wang Z, Deng Y, Qiao M, Peabody M, Zhang Q, Ye J, Yan Z, Denduluri S, Idowu O, Li M, Shen C, Hu A, Haydon RC, Kang R, Mok J, Lee MJ, Luu HL, Shi LL. Bone Morphogenetic Protein (BMP) signaling in development and human diseases. Genes & Diseases 2014;1:87–105.
42. Ali IHA, Brazil DP. Bone morphogenetic proteins and their antagonists: Current and emerging clinical uses. British Journal of Pharmacology 2014;171:3620–32.
43. Salazar VS, Gamer LW, Rosen V. BMP signalling in skeletal development, disease and repair. Nature Reviews Endocrinology 2016;12:203–21.
44. Zhang Y, Yang Y, Jiang M, Huang SX, Zhang W, Al Alam D, Danopoulos S, Mori M, Chen YW, Balasubramanian R, Chuva de Sousa Lopes SM, Serra C, Bialecka M, Kim E, Lin S, Toste de Carvalho ALR, Riccio PN, Cardoso WV, Zhang X, Snoeck HW, Que J. 3D Modeling of Esophageal Development using Human PSC-Derived Basal Progenitors Reveals a Critical Role for Notch Signaling. Cell Stem Cell 2018;23:516–29
45. Rodriguez P, Da Silva S, Oxburgh L, Wang F, Hogan BL, Que J. BMP signaling in the development of the mouse esophagus and forestomach. Development 2010;137:4171–6.
46. Hardwick JC, Van Den Brink GR, Bleuming SA, Ballester I, Van Den Brande JM, Keller JJ, Offerhaus GJ, Van Deventer SJ, Peppelenbosch MP. Bone morphogenetic protein 2 is expressed by, and acts upon, mature epithelial cells in the colon. Gastroenterology 2004;126:111–21.
47. Torihashi S, Hattori T, Hasegawa H, Kurahashi M, Ogaeri T, Fujimoto T. The expression and crucial roles of BMP signaling in development of smooth muscle progenitor cells in the mouse embryonic gut. Differentiation 2009;77:277–89.
48. Mulder DJ, Pacheco I, Hurlbut DJ, Mak N, Furuta GT, MacLeod RJ, Justinich CJ. FGF9-induced proliferative response to eosinophilic inflammation in oesophagitis. Gut

2009;58:166–73.

49. Iemura S, Yamamoto TS, Takagi C, Uchiyama H, Natsume T, Shimasaki S, Sugino H, Ueno N. Direct binding of follistatin to a complex of bone-morphogenetic protein and its receptor inhibits ventral and epidermal cell fates in early Xenopus embryo. Proceedings of the National Academy of Sciences of the United States of America 1998;95:9337.

50. Chandramouleeswaran PM, Shen D, Lee AJ, Benitez A, Dods K, Gambanga F, Wilkins BJ, Merves J, Noah Y, Toltzis S, Yearley JH, Spergel JM, Nakagawa H, Malefyt Rd, Muir AB, Wang ML. Preferential Secretion of Thymic Stromal Lymphopoietin (TSLP) by Terminally Differentiated Esophageal Epithelial Cells: Relevance to Eosinophilic Esophagitis (EoE). PLoS One 2016;11:e0150968.

51. Muir AB, Dods K, Noah Y, Toltzis S, Chandramouleeswaran PM, Lee A, Benitez A, Bedenbaugh A, Falk GW, Wells RG, Nakagawa H, Wang ML. Esophageal epithelial cells acquire functional characteristics of activated myofibroblasts after undergoing an epithelial to mesenchymal transition. Experimental Cell Research 2015;330:102–10.

52. Stuart T, Butler A, Hoffman P, Hafemeister C, Papalexi E, Mauck WM 3rd, Hao Y, Stoeckius M, Smibert P, Satija R. Comprehensive Integration of Single-Cell Data. Cell 2019;177:1888–902.

53. Waltman L, van Eck NJ. A smart local moving algorithm for large-scale modularity-based community detection. European Physical Journal B. 2013;86:471.

54. Cao J, Spielmann M, Qiu X, Huang X, Ibrahim DM, Hill AJ, Zhang F, Mundlos S, Christiansen L, Steemers FJ, Trapnell C, Shendure J. The single-cell transcriptional landscape of mammalian organogenesis. Nature. 2019;566:496–502.

55. Bray NL, Pimentel H, Melsted P, Pachter L. Near-optimal probabilistic RNA-seq quantification. Nature Biotechnology 2016;34:525–7.

56. Alexa A, Rahnenführer J, Lengauer T. Improved scoring of functional groups from gene expression data by decorrelating GO graph structure. Bioinformatics 2006;22:1600–7.

57. Mootha VK, Lindgren CM, Eriksson KF, Subramanian A, Sihag S, Lehar J, Puigserver P, Carlsson E, Ridderstråle M, Laurila E, Houstis N, Daly MJ, Patterson N, Mesirov JP, Golub TR, Tamayo P, Spiegelman B, Lander ES, Hirschhorn JN, Altshuler D, Groop LC. PGC-1α-responsive genes involved in oxidative phosphorylation are coordinately downregulated in human diabetes. Nature Genetics 2003;34:267–73.

58. Subramanian A, Tamayo P, Mootha VK, Mukherjee S, Ebert BL, Gillette MA, Paulovich A, Pomeroy SL, Golub TR, Lander ES, Mesirov JP. Gene set enrichment analysis: A knowledge-based approach for interpreting genome-wide expression profiles. Proceedings of the National Academy of Sciences of the United States of America 2005;102:15545–50.

59. Berggren WT, Lutz M, Modesto V. General spinfection protocol. In: The Stem Cell Research Community, eds. StemBook. Harvard Stem Cell Institute, 2008.

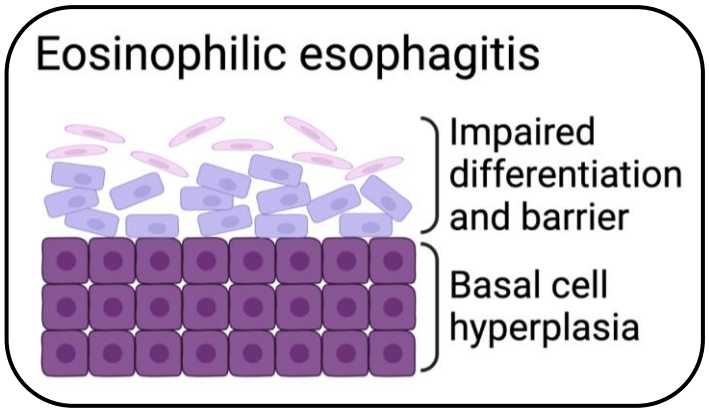
Eosinophilic esophagitis
Impaired differentiation and barrier
Basal cell hyperplasia

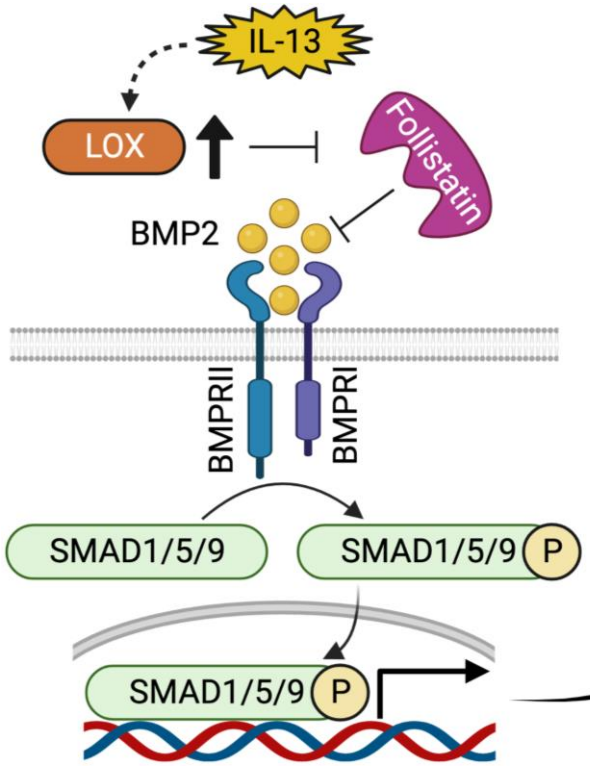
IL-13
LOX
Follistatin
BMP2
BMPRII
BMPRI
SMAD1/5/9
SMAD1/5/9 P
SMAD1/5/9 P

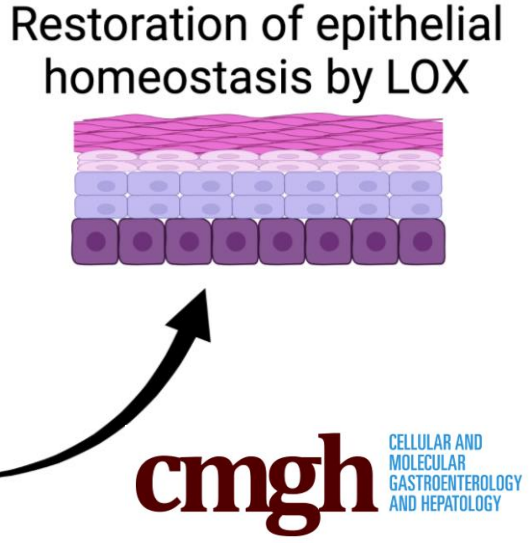
Restoration of epithelial homeostasis by LOX
cmgh
CELLULAR AND MOLECULAR GASTROENTEROLOGY AND HEPATOLOGY

Figure 1

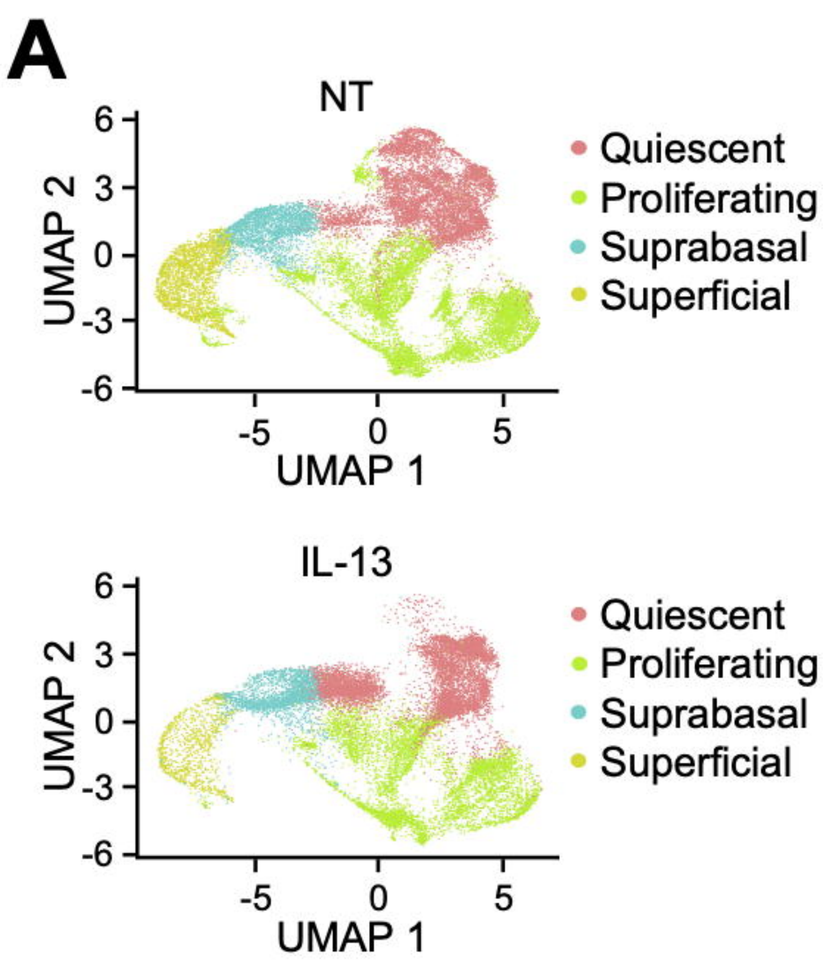

Figure 2

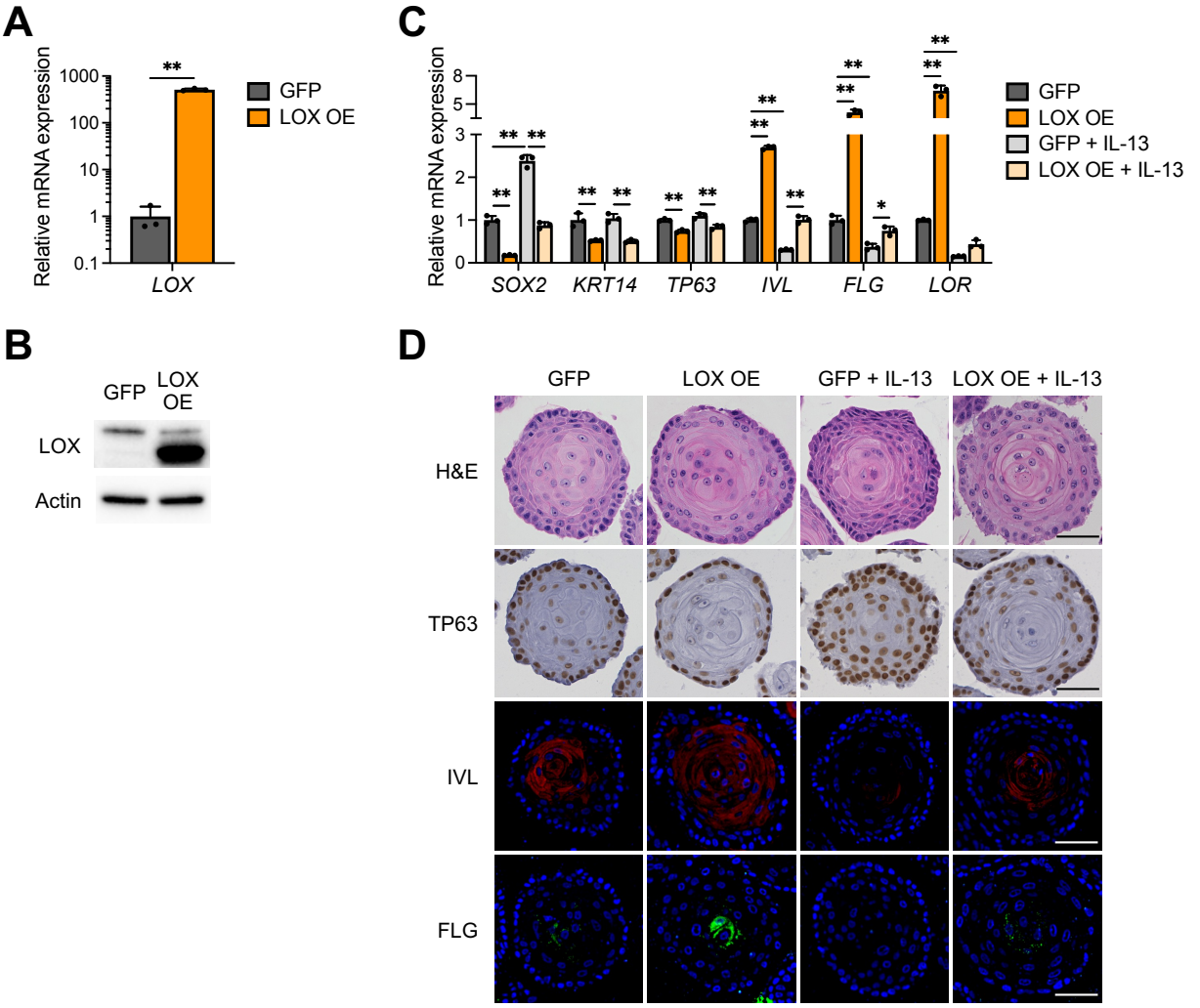

Figure 2. LOX overexpression promotes cell differentiation in esophageal epithelium.
(**A**) Quantitative RT-PCR for *LOX* of monolayer-cultured EPC2-hTERT cells overexpressing GFP or LOX (LOX OE) (n = 3). (**B**) Representative images of immunoblot for LOX of the monolayer-cultured GFP and LOX OE cells. (**C** and **D**) Alterations of aberrant LOX expression in EPC2-hTERT organoids. GFP and LOX OE organoids were stimulated with or without IL-13 (10 μg/ml) from day 7 to 11 and then harvested at day 11. (**C**) Quantitative RT-PCR for *SOX2*, *KRT14*, *TP63*, *IVL*, *FLG*, and *LOR* of the GFP and LOX OE organoids (n = 3). (**D**) Representative images of hematoxylin and eosin (H&E) staining, immunohistochemistry for TP63, and immunofluorescence staining for IVL (red) and FLG (green) of the GFP and LOX organoids. DAPI (blue). Scale bar, 50 μm. Data are representative of three independent experiments and expressed as means ± SDs. Two-tailed Student's t-test (**A**) and one-way analysis of variance (**C**) were performed for statistical analyses. $*P < 0.05$, $**P < 0.01$.

Figure 3

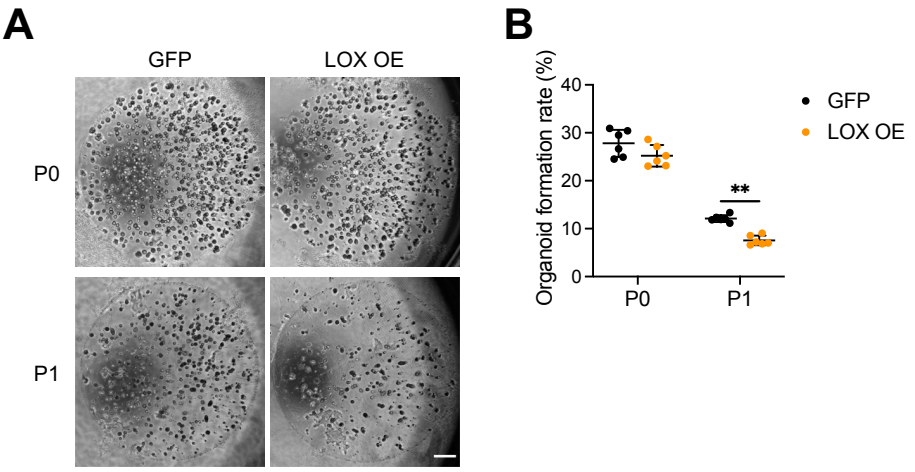

Figure 3. LOX overexpression attenuates organoid formation capacity.
(**A**) Representative phase contrast images of EPC2-hTERT organoids overexpressing GFP or LOX (LOX OE) at day 11. Organoid formation rate (OFR) was assessed at day 11 (P0) and they were then passaged. OFR was assessed again at day 11 (P1). Scale bar, 50 μm. (**B**) OFR was defined as the number of organoids (≥ 50 μm) divided by the total seeded cells. Data are representative of three independent experiments and expressed as means ± SDs (n = 6). Two-tailed Student's t-test was performed for statistical analyses. $^{**}P < 0.01$.

Figure 4

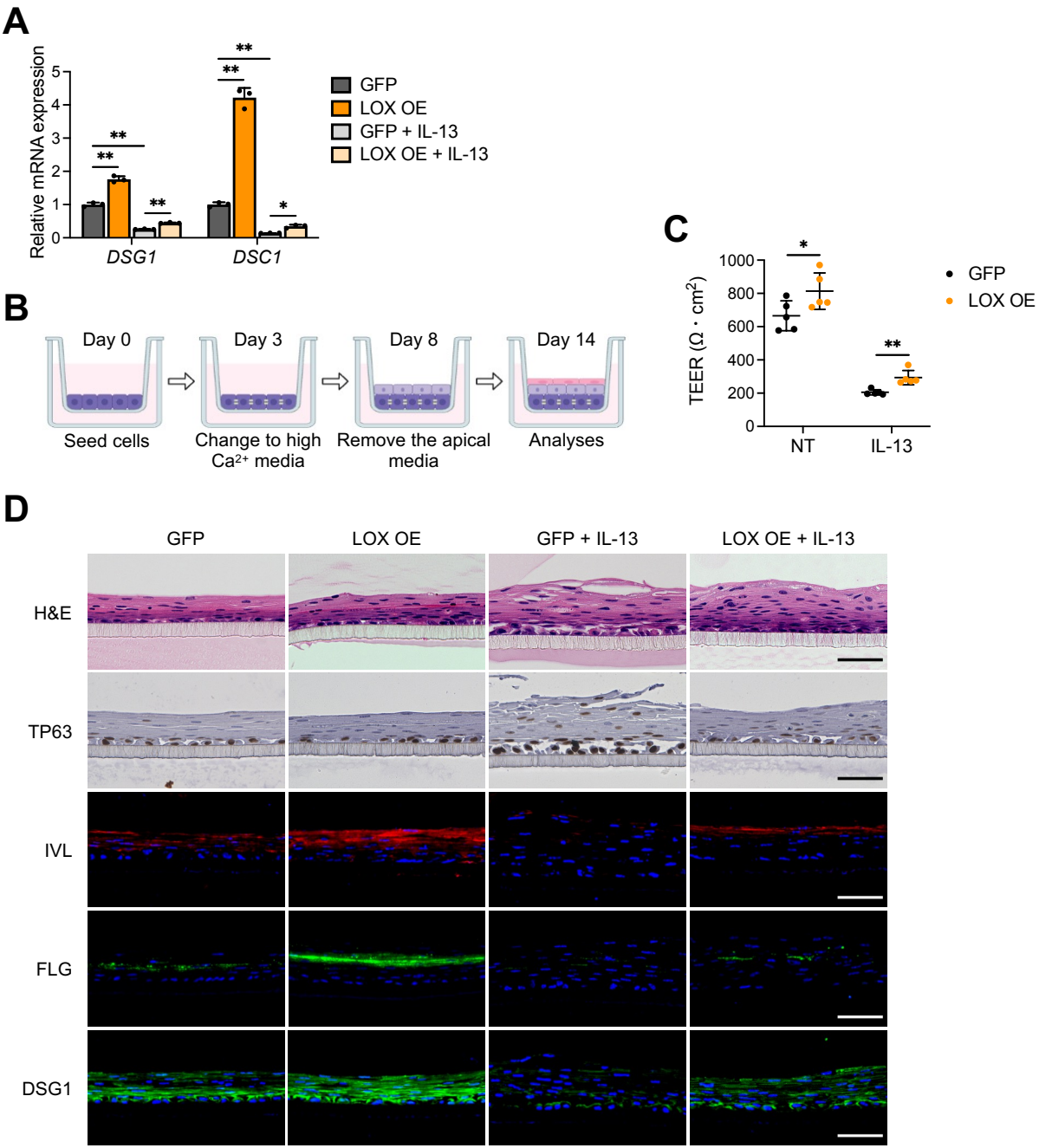

Figure 4. LOX overexpression improves epithelial barrier integrity.
(**A**) Quantitative RT-PCR for *DSG1* and *DSC1* of EPC2-hTERT organoids overexpressing GFP or LOX (LOX OE). GFP and LOX OE organoids were stimulated with or without IL-13 (10 μg/ml) from day 7 to 11 and then harvested at day 11 (n = 3). Data are representative of three independent experiments. (**B**) Schematic of air-liquid interface (ALI) model. GFP and LOX OE EPC2-hTERT cells were cultured in low-calcium (0.09 mM Ca2+) media for 3 days, followed by high-calcium media (1.8 mM Ca2+) for 5 days, and then brought to ALI at day 8. ALI-cultured cells were stimulated with or without IL-13 (10 μg/ml) from day 9 to 14. (**C**) Transepithelial electrical resistance (TEER, Ω * cm2) in the GFP and LOX OE EPC2-hTERT ALI-cultures (n = 5). (**D**) Representative images of hematoxylin and eosin (H&E), immunohistochemistry for TP63, and immunofluorescence staining for IVL (red), FLG (green), and DSG1 (green) of the GFP and LOX OE EPC2-hTERT ALI-cultures. DAPI (blue). Scale bar, 50 μm. Data are representative of two independent experiments and expressed as means ± SDs. One-way analysis of variance (**A**) and two-tailed Student's t-test (**C**) were performed for statistical analyses. *$P < 0.05$, **$P < 0.01$. NT, nontreated.

Figure 5

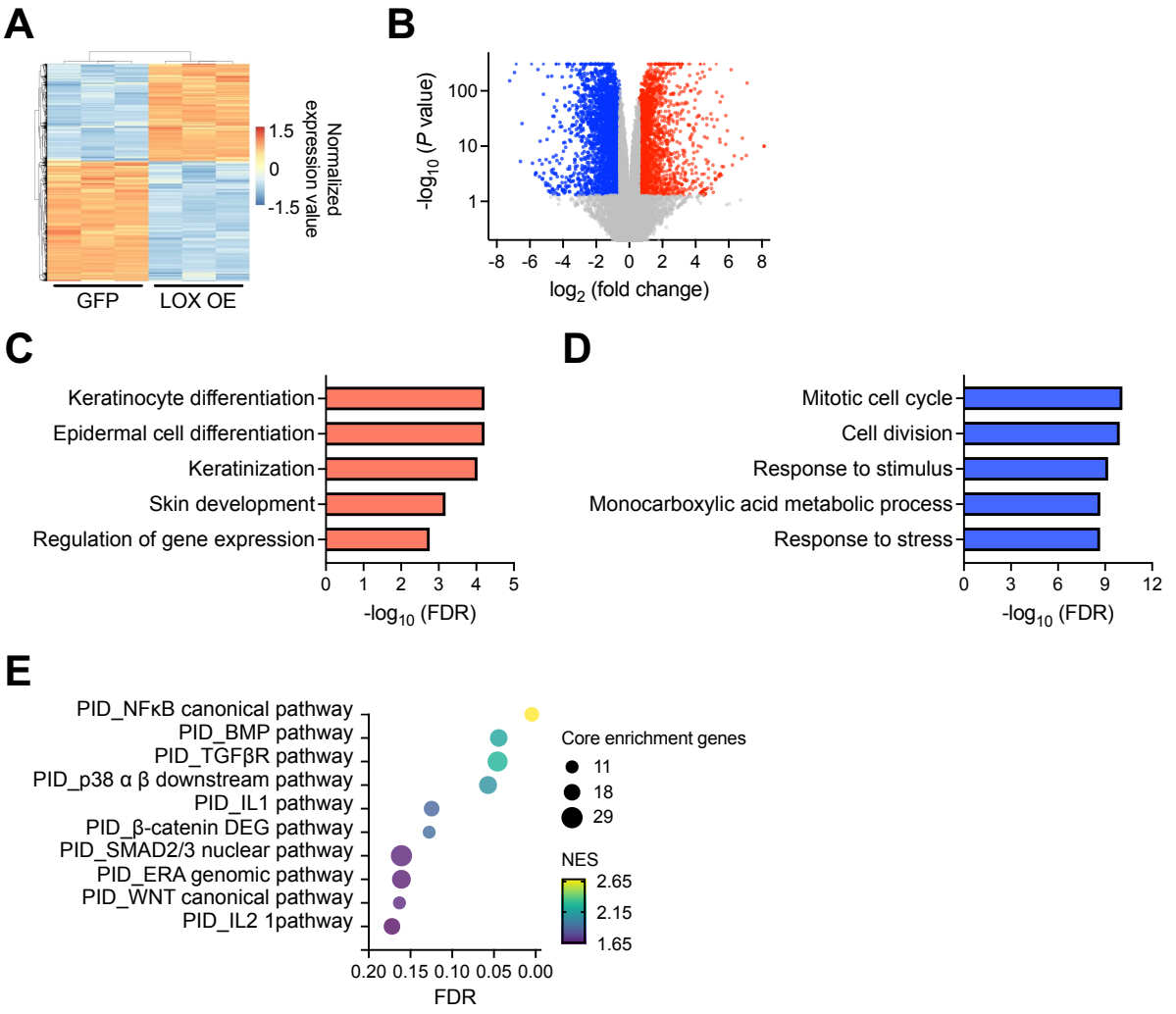

Figure 5. Transcriptome analysis identifies the functional roles of LOX in esophageal epithelium.
(**A**) Heatmap and (**B**) volcano plot of differentially expressed genes (DEGs) based on RNA sequencing data from EPC2-hTERT organoids overexpressing GFP or LOX (LOX OE). GFP and LOX OE organoids were cultured for 11 days and subjected to RNA sequencing analysis. Upregulated and downregulated DEGs in LOX OE organoids are shown with red and blue, respectively. (**C** and **D**) Top 5 enriched (**C**) and depleted (**D**) terms in LOX OE organoids based on Gene Ontology analysis. (**E**) Gene Set Enrichment Analysis based on the Pathway Interaction Database (PID). Top 10 enriched pathways in LOX OE organoids are shown. Dot size and color represent the number of core enrichment genes and normalized enrichment score (NES) in the pathway, respectively. FDR, false discovery rate.

Figure 6

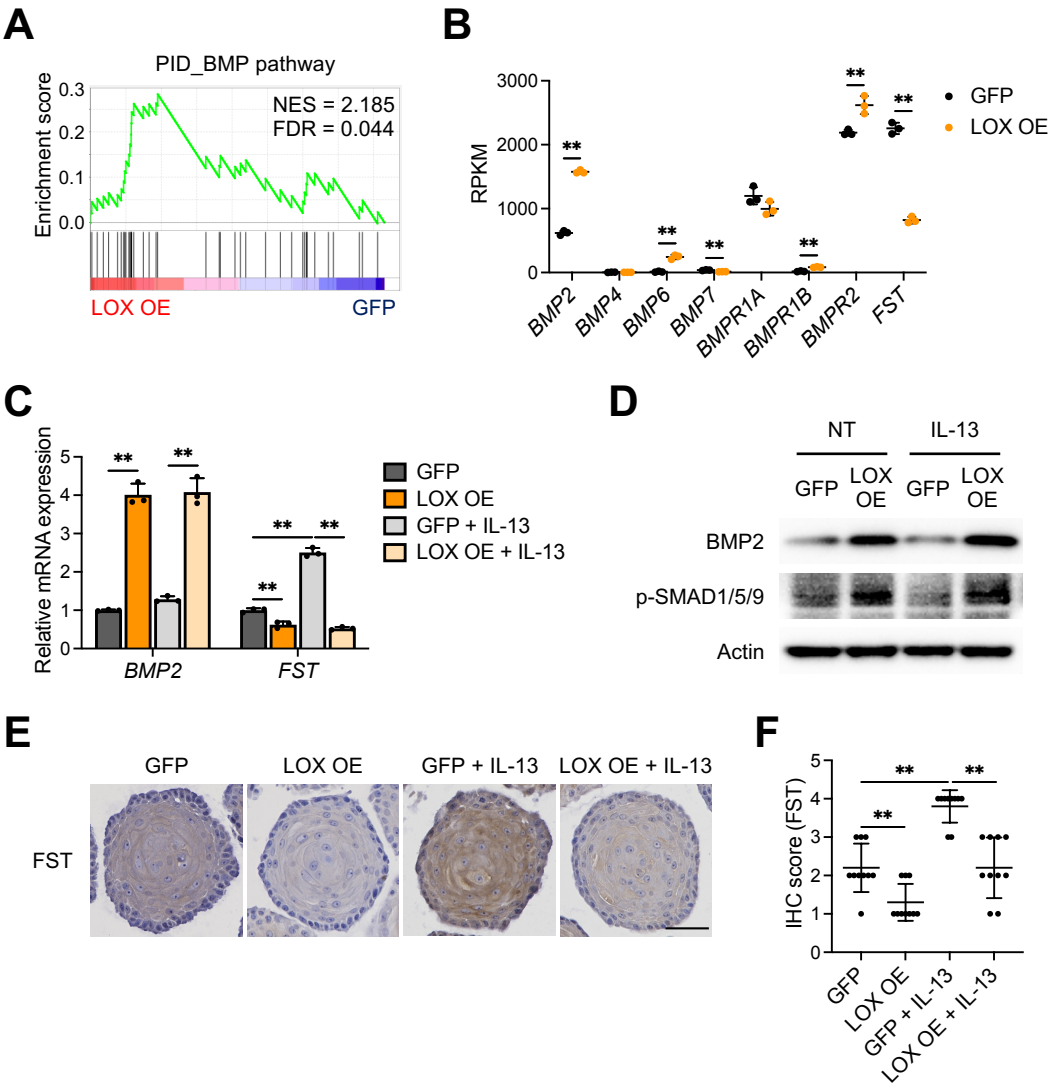

Figure 6. BMP signaling pathway is activated in LOX overexpressing organoids.
(**A**) Gene Set Enrichment Analysis for BMP pathway in the Pathway Interaction Database (PID) based on the LOX overexpressing (LOX OE) organoids RNA sequencing data. (**B**) Expression of BMP and BMP receptor (BMPR) genes which relevant to the BMP pathway gene set, plotted as reads per kilobase per million (RPKM) (n = 3). (**C**-**F**) Validation of the BMP activation in EPC2-hTERT organoids. GFP and LOX OE organoids were cultured with or without IL-13 (10 μg/ml) from day 7 to 11 and then harvested at day 11. (**C**) Quantitative RT-PCR for *BMP2* and *FST* of the GFP and LOX OE organoids (n = 3). (**D**) Representative images of immunoblot for BMP2 and phospho-SMAD1/5/9 (p-SMAD1/5/9) and (**E**) immunohistochemistry staining for FST of the GFP and LOX OE organoids. Scale bar, 50 μm. (**F**) FST protein levels were quantified with the scoring described in the method (n = 10). Data are representative of three independent experiments and expressed as means ± SDs. Two-tailed Student's t-test (**B**) and one-way analysis of variance (**C** and **F**) were performed for statistical analyses. $^{**}P < 0.01$. FDR, false discovery rate; NES, normalized enrichment score; NT, nontreated.

Figure 7

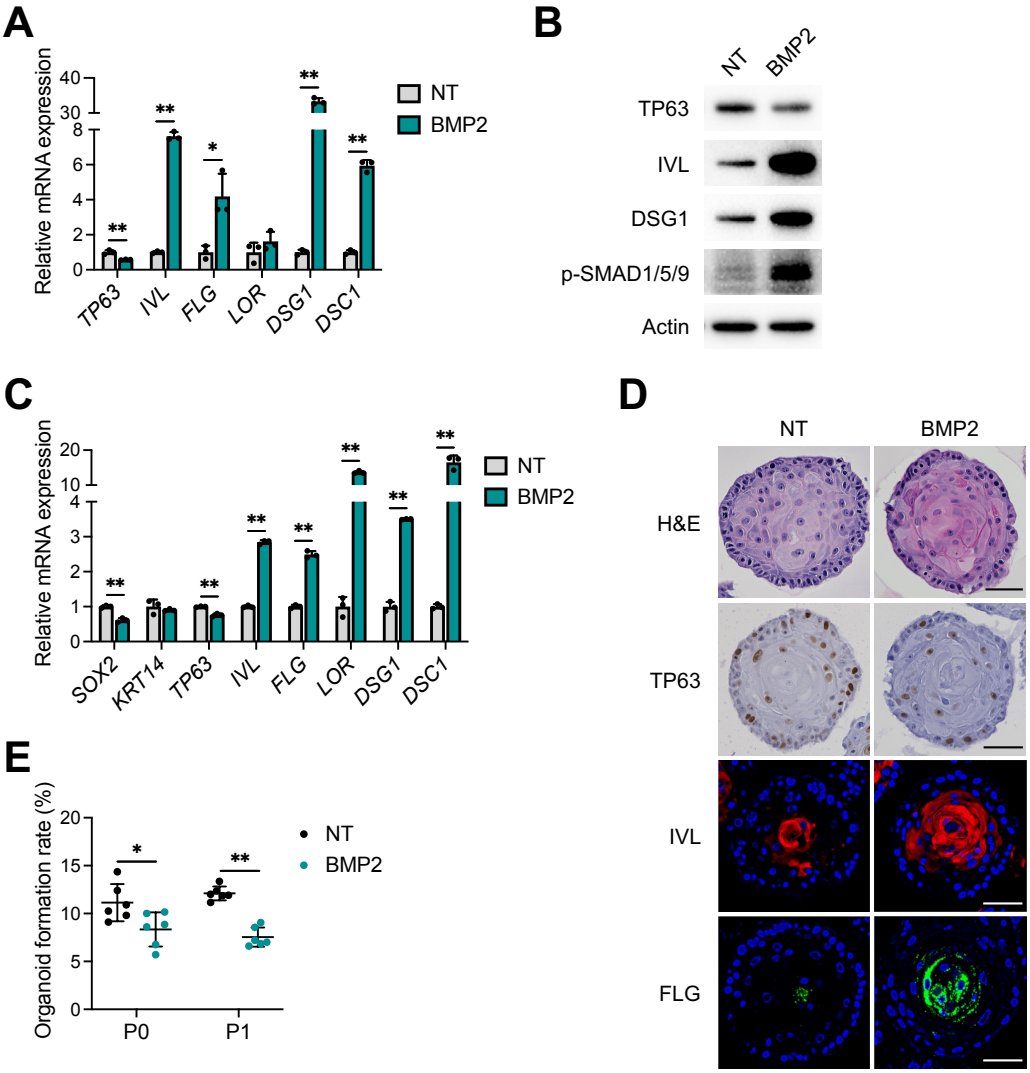

Figure 7. BMP2 treatment induces cell differentiation in esophageal epithelium.
(**A** and **B**) BMP2 treatment in monolayer culture of EPC2-hTERT cells. EPC2-hTERT cells were treated with recombinant BMP2 protein (10 μg/ml) for 72 h in high-calcium (1.8 mM Ca^{2+}) media. (**A**) Quantitative RT-PCR for *TP63*, *IVL*, *FLG*, *LOR*, *DSG1*, and *DSC1* in the EPC2-hTERT cells (n = 3). (**B**) Representative images of immunoblot for TP63, IVL, DSG1, and phospho-SMAD1/5/9 (p-SMAD1/5/9) of the EPC2-hTERT cells. (**C**-**E**) EPC2-hTERT organoids were treated with recombinant BMP2 protein (10 μg/ml) from day 7 to 11 and then harvested at day 11. (**C**) Quantitative RT-PCR for *SOX2*, *KRT14*, *TP63*, *IVL*, *FLG*, *LOR*, *DSG1*, and *DSC1* in the EPC2-hTERT organoids (n = 3). (**D**) Representative images of hematoxylin and eosin (H&E) staining, immunohistochemistry for TP63, and immunofluorescence staining for IVL (red) and FLG (green) of the EPC2-hTERT organoids. DAPI (blue). Scale bar, 50 μm. (**E**) Organoid formation rate (OFR) was assessed at day 11 (P0) and they were then passaged. OFR was assessed again at day 11 (P1). OFR was defined as the number of organoids (≥ 50 μm) divided by the total seeded cells (n = 6). Data are representative of three independent experiments and expressed as means ± SDs. Two-tailed Student's t-test (**A**, **C**, and **E**) was performed for statistical analyses. *P < 0.05, **P < 0.01. NT, nontreated.